Chemical Science

Accepted Manuscript

This article can be cited before page numbers have been issued, to do this please use: X. Fu, B. Xu, H. Liyanage, C. Zhang, W. F. Kincaid, A. L. Ford, L. G. Westbrook, S. D. Brown, T. DeMarco, J. Hougland, J. M. Franck and X. Hu, *Chem. Sci.*, 2025, DOI: 10.1039/D5SC05710H.

ROYAL SOCIETY OF CHEMISTRY

rsc.li/chemical-science

View Article Online
DOI: 10.1039/D5SC05710H

ARTICLE

Ultrasound-Triggered Prodrug Activation via Sonochemically Induced Cleavage of a 3,5-Dihydroxybenzyl Carbamate Scaffold

Received 00th January 20xx,
Accepted 00th January 20xx

DOI: 10.1039/x0xx00000x

Xuancheng Fu,[a] Bowen Xu,[a] Hirusha Liyanage,[a] Cijun Zhang,[a] Warren F. Kincaid,[a] Amber L. Ford,[a] Luke G. Westbrook,[a] Seth D. Brown,[a] Tatum DeMarco,[a] James L. Hougland,[a,b] John M. Franck,[a] Xiaoran Hu*[a]

Spatiotemporal control of drug release in deep tissues is crucial for targeted treatment precision and minimized systemic side effects. Ultrasound is a non-invasive and clinically safe stimulus capable of deep-tissue penetration without requiring optical transparency. Here, we introduce an innovative strategy for controlling cargo release via ultrasound-triggered sonochemical cleavage of a 3,5-dihydroxybenzyl carbamate (DHBC) prodrug platform. We demonstrate that low-intensity therapeutic ultrasound (LITUS) effectively generates hydroxyl radicals in aqueous solutions, which hydroxylate DHBC to initiate spontaneous cleavage and cargo release. Using a prototype chemotherapy prodrug (**ProDOX**) as a proof-of-concept, we show that LITUS irradiation triggers doxorubicin release to kill cancer cells in vitro. Remarkably, this sonochemical activation was successfully achieved through 2 cm of chicken breast, highlighting the deep-penetrating capability of our approach. Extending this strategy, we developed **ProR848**, a sono-activable prodrug of the Toll-like receptors (TLR) agonist R848, enabling remotely triggered, on-demand immune cell activation. Collectively, our results establish a novel and versatile sonochemical cleavage platform for ultrasound-targeted prodrug activation, offering significant potential for applications including controlled therapeutic release and responsive biomaterials

Introduction

Achieving spatiotemporal control over cleavage chemistries deep within biological tissues is critically important for biomedical applications, such as site-specific drug release and dynamically tunable biomaterials.[1–3] However, current methods for remotely controlling chemical bond cleavage in deep tissue remain limited. Photo-responsive chemistry has been widely used to control drug release in vitro and on skin surfaces, but the limitation of tissue penetration hampers its application in deep tissues.[4,5] Radiation-controlled drug release has received increasing attention due to its deep-penetrating ability,[6–8] but it requires specialized equipment, and managing radiotherapy-associated side effects remains a significant concern. Ultrasound (U/S), mechanical sound waves beyond human hearing (20 kHz to MHz range), is widely used in biomedical fields such as deep-tissue imaging and oncology treatment.[9–12] Ultrasound as a stimulus features a unique combination of advantages: it operates remotely and non-invasively, penetrates deep tissues without needing optical transparency, offers precise targeting, and utilizes cost-effective setups that have been proven safe in clinical applications.

Conventional ultrasound-targeted drug delivery systems harness the physical effects of acoustic waves, such as sonoporation (i.e., ultrasound-induced formation of transient pores in cell membranes, improving membrane permeability) and enhanced extravasation, to improve local pharmacokinetics and drug biodistribution.[13] However, the utilization of active drugs still poses a risk of off-target side effects. An emerging strategy[14] addresses this challenge by employing ultrasound-controlled cleavage chemistry (**Figure 1**) to activate covalently modified, nontoxic prodrugs exclusively at the target site, enabling localized activation of therapeutic effects while minimizing systemic drug exposure. One such approach (**Figure 1a**) utilizes the sonodynamic effect (i.e., ultrasonic generation of reactive oxygen species from sonosensitizers[15–21]) to induce chemical transformations for drug release.[22–26] However, the requirement for sonosensitizers increases formulation complexity in sonodynamic-based prodrug delivery systems. On the other hand, another ultrasound-mediated bond cleavage strategy (**Figure 1b**) leverages the ultrasound-induced shear force field in solution to mechano-chemically activate force-sensitive structures, resulting in bond cleavage and cargo release.[27–33] Despite recent advancements in the field,[34–36] conventional polymer-mechanochemistry approaches often involve harsh, high-intensity ultrasonication conditions and necessitate the incorporation of long polymers to prodrug structures (restricting drug loading to <1 wt%), presenting challenges for clinical applicability.

Ultrasound-induced generation of hydroxyl radicals (·OH) in aqueous environments is a well-established phenomenon in sonochemistry.[37–43] Clinical acoustic conditions are known to cause acoustic cavitation both in vivo and in vitro.[44–47] This

[a] Department of Chemistry, BioInspired Institute, Syracuse University, Syracuse, New York, 13244, United States
[b] Department of Biology, Syracuse University, Syracuse, New York, 13244, United States

cavitation bubble, essentially a vacuum, collapses near-adiabatically and results in extreme pressures over 1000 atm and temperatures above 5000 K, while only slightly affecting the temperature of the bulk liquid. The extreme cavitation environment in collapsing cavitation bubbles serves as sonochemical micro-reactors and is sufficient to cause the pyrolysis of vapor molecules trapped in the bubble, generating primary radicals.[48–51] For example, Riesz used the methods of spin trapping electron spin resonance (ESR) to directly observe the formation of ·OH and ·H in the cavitation bubbles.[42,47,52,53] These primary radicals can either recombine or diffuse from the gas phase into the vicinity of the bubble and induce a wide variety of secondary chemical reactions in the bulk solution.[54–60] However, applying these intrinsic chemical effects of ultrasound to drive predictable and constructive chemistry for biomedical applications remains an underexplored yet potentially transformative research venue.[61]

The hydroxyl radical (·OH), with a Hammett σ value of -0.41,[62] is known to undergo electrophilic substitution reactions, and its ability to hydroxylate aromatic compounds has been studied primarily using ·OH generated by Fenton's reagent[63,64] or water radiolysis.[65–67] Recently, Liu and coworkers elegantly harnessed ·OH produced from radiolysis to hydroxylate an electron-rich 3,5-dihydroxybenzyl carbamate, triggering cascade chemical transformations that lead to the release of covalently conjugated drugs.[65] Inspired by ultrasound's intrinsic ability to generate ·OH radicals and the reactivity of ·OH in mediating radical hydroxylation,[50,65] we have developed a sonochemically controlled cleavage platform based on a 3,5-dihydroxybenzyl carbamate (DHBC) prodrug scaffold (**Figure 1c**). Using a commercially available, FDA-registered low-intensity therapeutic ultrasound (LITUS) device, sonochemically generated ·OH radicals react with the DHBC via radical hydroxylation, triggering a subsequent elimination cascade that releases the molecular cargo. As a proof-of-concept, we synthesized a model prodrug **ProDOX** incorporating a chemotherapy drug doxorubicin (DOX), which is selectively activated under LITUS to release DOX and kill cancer cells in vitro. To demonstrate the deep-penetration ability of our strategy, we successfully activated **ProDOX** through a 2-cm thick chicken breast. Further, we extended the platform to immunotherapy by developing **ProR848**, a sono-activable prodrug of the toll-like receptor (TLR) agonist R848, designed to mitigate the systemic toxicity associated with TLR-based treatments. Upon LITUS irradiation, **ProR848** released active R848, selectively activating tumor-associated macrophages (TAMs) and dendritic cells (DCs), as evidenced by upregulation of pro-inflammatory markers and inflammatory cytokine secretion. Together, these chemotherapeutic and immunotherapeutic applications demonstrate the versatility and effectiveness of our deep-penetrating, ultrasound-triggered cleavage platform, offering significant potential for applications ranging from controlled therapeutic release to responsive biomaterials.

Results and Discussion

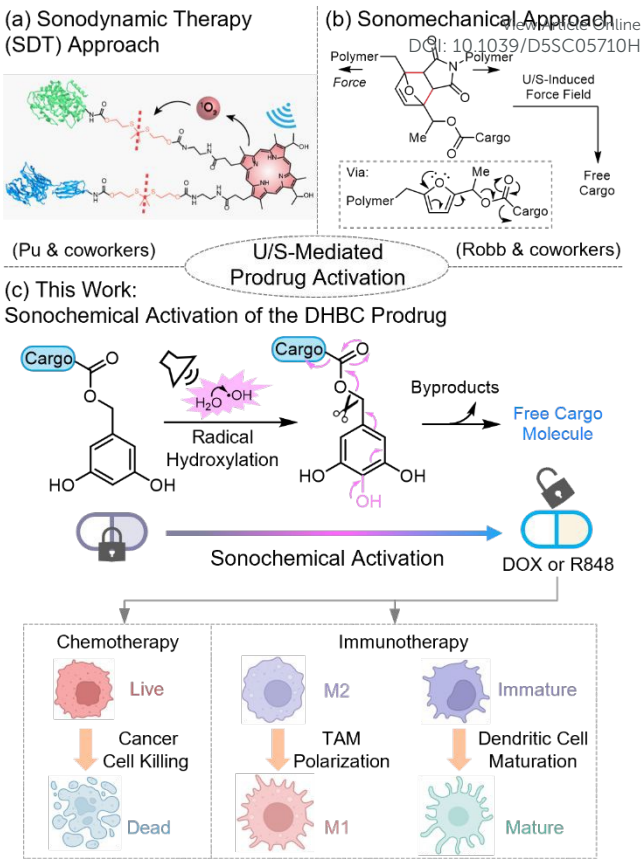

Fig. 1 An overview of ultrasound-mediated prodrug activation strategies. This work introduces a sonochemical approach that harnesses the intrinsic chemical effects of ultrasound in aqueous solutions to activate DHBC prodrugs via a radical hydroxylation mechanism. Figure 1a is adapted with permission from ref 24. Copyright 2022, Springer Nature.

We first investigated the sonochemical production of ·OH radicals using an FDA-registered, commercially available ultrasound device. Under our standard LITUS conditions (frequency: 1 MHz; power: 1.0 W/cm^2; duty cycle: 50%) (see SI for mechanical index calculations and biosafety discussions), the generation of ·OH in the acoustically irradiated PBS buffer solutions was monitored using ESR with 5,5-dimethyl-1-pyrroline-N-oxide (DMPO), a ·OH-specific spin trap that forms a well-understood DMPO-OH spin adduct in presence of ·OH radicals.[53] LITUS irradiation produced a new set of four-line peaks (**Figure 2a**) which are characteristic of the hyperfine coupling in the DMPO–OH adduct, while DMPO–OOH signals were not seen. Comparison with reported hyperfine coupling constants[68] as well as simulated ESR spectrum (Figure S1) confirms that these new peaks correspond to the expected DMPO-OH spin adduct. From ESR spin-counting analysis (see SI for details), the concentration of DMPO-OH was determined to be 18.8 μM after 5 min sonication of a 5 mM DMPO solution.

We further performed a quantitative study of ultrasonic ·OH generation using an established terephthalic acid (TA) dosimetry method—the nonfluorescent TA readily reacts with ·OH to yield fluorescent 2-hydroxy terephthalic acid (hTA).[69,70] The fluorescence emission of an irradiated TA solution linearly increased in the first five minutes of ultrasonication (**Figure 2b**

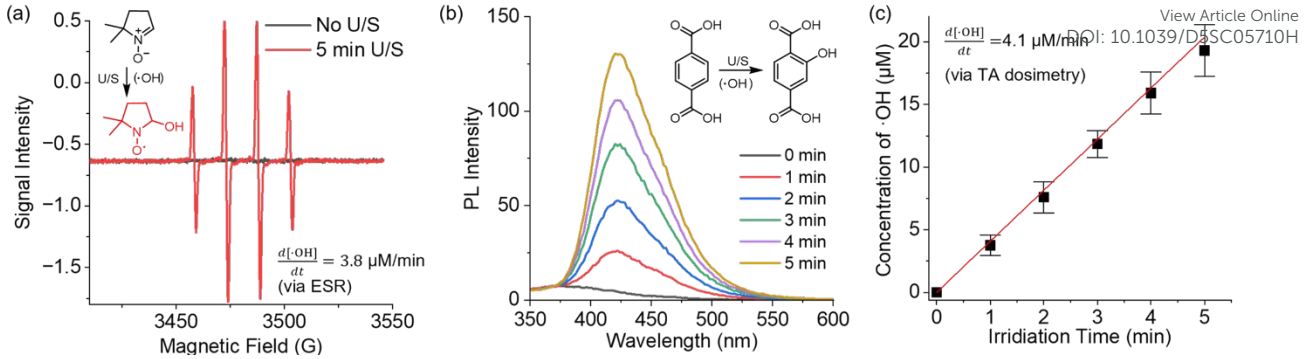

Fig. 2 (a) ESR spectra of a 5 mM solution of DMPO in PBS before and after sonication. (b) Sonochemical conversion of TA (20 mM in PBS) to hTA monitored by fluorescence spectroscopy. (c) Concentration of sonochemical ·OH as a function of sonication time, calculated by multiplying the concentration of hTA by 1/0.35.

and **2c**), indicating the steady sonochemical conversion of TA to hTA. It is understood that about 35% of sonochemical ·OH radicals react with TA to produce hTA,[71,72] and therefore, the concentration of ·OH produced in 5 minutes of ultrasonication was calculated to be 20.4 μM (4.1 μM/min), which aligns closely with that estimated by ESR. To confirm the radical nature of the observed hydroxylation of TA, we conducted a control experiment using a highly reactive radical quencher, hydroquinone (rate constant of 11×10^9 M^{-1} s^{-1} with ·OH).[73] The addition of 100 mM hydroquinone into a 20 mM TA solution near completely inhibited TA hydroxylation, confirming the key role of radicals (**Figure S5**).

Following the sonochemical TA dosimetry experiments, we explored the potential of harnessing sonochemical ·OH to trigger the radical hydroxylation and cascade molecular release from a DHBC-based model prodrug **Pro1**. Electron-rich DHBC motifs are designed to react with sonochemically generated ·OH through a radicalphilic reaction, triggering a cascade elimination process that releases the 4-nitroaniline payload (**Figure 3a**).[65] The release of 4-nitroaniline results in the emergence of a characteristic absorption around 400 nm, providing a convenient signal for monitoring its release using UV-vis spectroscopy. As shown in **Figure 3b**, ultrasound irradiation of a 50 μM solution of **Pro1** in PBS results in an absorbance increase around 400 nm, corresponding to nitroaniline release. HPLC measurements further confirmed the identity of 4-nitroaniline (**Figure 3c**). The rate of 4-nitroaniline release in the first 5 min was estimated at 2.4 μM/min based on absorbance measurements (**Figure 3d**), indicating this model DHBC prodrug was effectively activated under our sonochemical conditions to release the cargo molecules. The release of 4-nitroaniline plateaued at approximately 22 μM after 20-min sonication (**Figure S8**). The incomplete conversion is anticipated due to nonspecific sonochemical side reactions—sonochemical degradation of both **Pro1** and the released nitroaniline can occur in or near the cavitation microbubbles, which feature extreme environments. Currently, we are unable to identify the sonochemical byproduct(s).

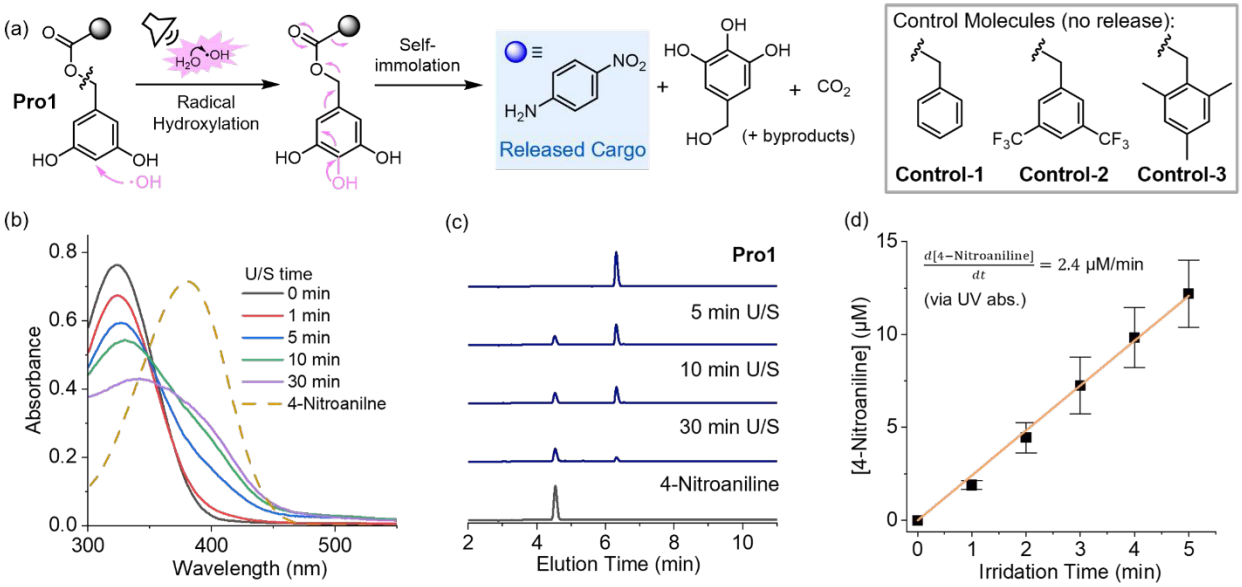

Fig. 3 (a) Ultrasonic activation of **Pro1** mediated by sonochemical ·OH radicals. For simplicity, only the hydroxylation reaction at the 4-position is depicted, although hydroxylation at the 2-position is also possible (**Figure S6**).[65] Structures of control molecules are also shown. (b) Absorption spectra of a 50 μM solution of **Pro1** in PBS as a function of sonication time. The dashed curve corresponds to the absorbance of a separately prepared 50 μM solution of 4-nitroaniline. (c) Sonolysis of **Pro1** monitored by HPLC. (d) The concentration of free 4-nitroaniline in the **Pro1** solution in the first 5 minutes of ultrasound irradiation, calculated from the absorbance increase at 400 nm.

View Article Online
DOI: 10.1039/D5SC05710H

We conducted a series of control experiments to validate the proposed sonolysis mechanism. By introducing 100 mM hydroquinone (radical quencher) into the **Pro1** solution, ultrasound-triggered cargo release from **Pro1** was inhibited (**Figure S10**), supporting that the observed sonochemical activation of **Pro1** is through a radical mechanism. Additionally, we designed **Control-1/2/3** molecules where the electron-rich 3,5-dihydroxybenzyl motif was replaced: **Control-1** and **Control-2** contain a less ·OH-reactive benzyl motif and 3,5-bis(trifluoromethyl)benzyl motif, respectively, while **Control-3** comprises a 2,4,6-trimethylbenzyl group, whose hydroxylation product is inactive toward the elimination cascade (**Figure S12**). Irradiation of **Control-1/2/3** molecules under identical acoustic conditions as used for **Pro1** lead to minor increase in 4-nitroaniline absorbance (**Figure S11**). HPLC analysis also confirmed the absence of cargo release from sonicated control molecules (**Figure S12**).

As a proof of concept, we demonstrated ultrasound-triggered release of a cytotoxic chemotherapy drug DOX from the sonochemically responsive DHBC prodrug platform (**Figure 4a**). This prototype model prodrug **ProDOX** was exposed to standard LITUS irradiation, with the reaction monitored by HPLC equipped with a UV detector (monitored at 254 nm). The sonicated solutions displayed a distinct peak at around 4.3 min elution time, corresponding to free DOX released from the activated prodrug (**Figure S14**). The DOX peak steadily increased during the first five minutes of ultrasonication, reaching a peak concentration of around 0.5 μM. However, prolonged sonication reduced the DOX concentration, presumably due to the nonspecific sonolysis of DOX under cavitational conditions (**Figure 4b**). The appearance of the inflection point for DOX

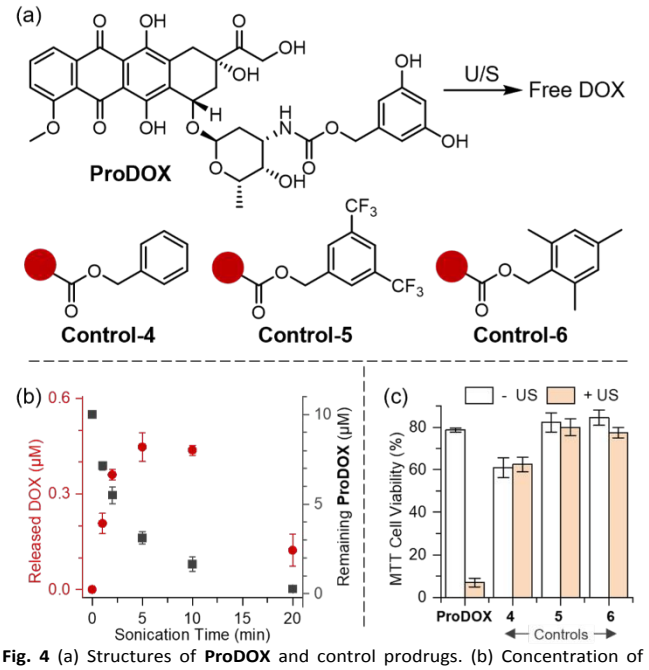

Fig. 4 (a) Structures of **ProDOX** and control prodrugs. (b) Concentration of released DOX from a solution of 10 μM **ProDOX** in PBS as a function of sonication time. (c) MTT viability assay results demonstrate increased cytotoxicity in LITUS-irradiated **ProDOX** solution, compared to a nonirradiated **ProDOX** solution. This ultrasound-induced cytotoxicity is not observed in control prodrugs.

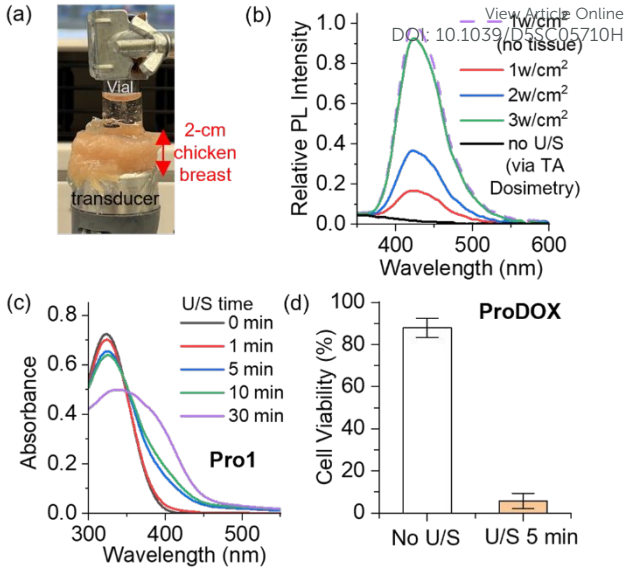

Fig. 5 (a) A photograph showing our setup applying LITUS through a 2 cm thick chicken breast tissue to a solution. (b) Fluorescence spectra of 20 mM TA solutions after 5 min of LITUS irradiation at varied sound intensity (1 MHz, 50% duty cycle) applied through chicken breast. All traces are normalized relative to the fluorescence of a TA solution sonicated (1 W/cm², 5min) without chicken breast (dashed line). (c) Absorption spectra monitoring the release of 4-nitroaniline from a 50 μM **Pro1** solution as a function of sonication (3 W/cm², through chicken breast). (d) MTT viability assay with *HeLa* cells show LITUS-induced (3 W/cm², through chicken breast) cytotoxicity of **ProDOX**

concentration matches the trend observed for 4-nitroaniline release from **Pro1** (Figure S8). Given the electron-rich, anthraquinone structure of DOX, it is particularly susceptible to non-specific degradation under sonochemical conditions (**Figure S15**).

While future research will explore the structure-activity relationships affecting the sonochemical stability of therapeutically active structures and will identify candidates with enhanced resistance to sonolysis, the efficacy of our current prototype model prodrug is sufficient to demonstrate the ultrasound-controlled DOX release for in vitro cancer treatment. *HeLa* cells were treated in vitro by solutions of **ProDOX**, with or without ultrasonic irradiation (**Figure 4c**, left). Only the sonicated **ProDOX** (yellow bar) exhibited significant cytotoxicity, confirming that ultrasonic irradiation activated the cytotoxicity of **ProDOX**. Meanwhile, control groups with DOX masked by various benzyl derivatives showed limited toxicity both in the presence and in the absence of sonication, with HPLC confirming no DOX release (**Figure S14**).

Then, we demonstrate the tissue-penetration ability of our controlled-release techniques by remotely manipulating the chemical transformation of prodrugs using LITUS through a 2-cm-thick chicken breast (**Figure 5a**). Through the animal tissue, our standard 1 W/cm² LITUS condition successfully triggered the hydroxylation of TA as indicated by fluorescence turn-on, while moderately increased acoustic intensity at 3 W/cm² exhibits more pronounced sonochemical effects (**Figure 5b**)–this 3 W/cm² intensity was used in all tissue-penetrating experiments. Ultrasound irradiation applied through the chicken breast successfully triggered the release of 4-nitroaniline from **Pro1** (**Figure 5c**) as well as DOX from **ProDOX**

View Article Online
DOI: 10.1039/D5SC05710H

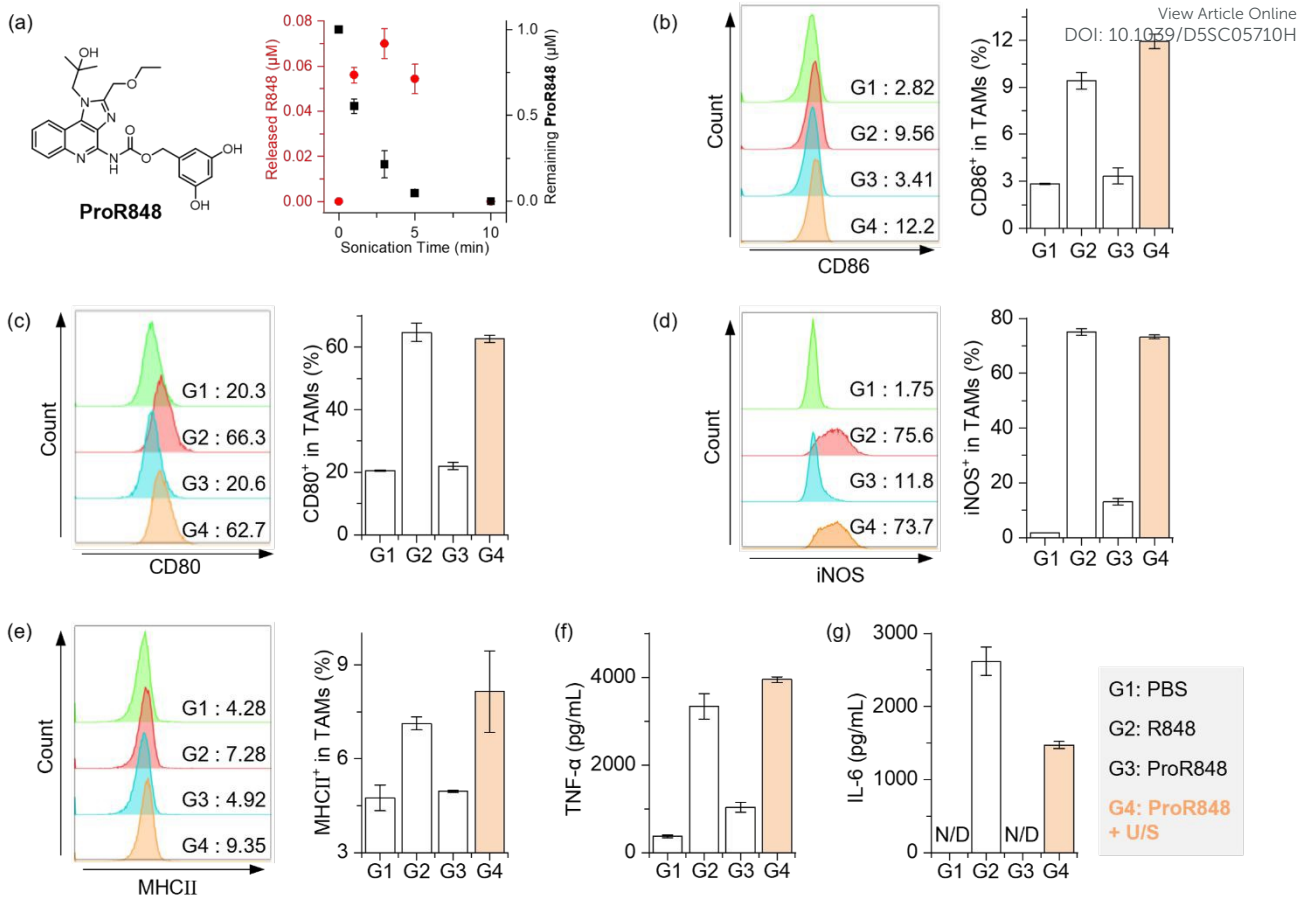

Fig. 6 (a) Structures of **ProR848** and concentration of released R848 from a solution of 1 μM **ProR848** in PBS as a function of sonication time (1 MHz, 50% duty cycle, 1 W/cm²), quantified by HPLC. (b–e) Flow cytometry analysis showing enhanced expression of pro-inflammatory markers on tumor-associated macrophages (TAMs) after treatment with **ProR848** activated by 3 min ultrasound irradiation (G4, orange bars), compared with PBS negative control (G1), free R848 positive control (0.07 μM, G2), and non-sonicated **ProR848** (G3): (b) CD86, (c) CD80, (d) iNOS, (e) MHC class II. (f,g) ELISA measurements demonstrating secretion of pro-inflammatory cytokines from TAM supernatants after various treatments (G1 to G4): (f) TNF-α, (g) IL-6.

(**Figure S18**). Ultrasound applied through chicken breast effectively activated **ProDOX** solutions, enhancing their cytotoxicity against *HeLa* cells in vitro (**Figure 5d**).

TLR agonists represent potent immunotherapeutic agents capable of enhancing immune activation and remodeling immunosuppressive tumor microenvironments.[74,75] This effect is primarily mediated through the activation of immune cells, particularly by polarizing tumor-associated macrophages (TAMs) from an anti-inflammatory, pro-tumoral M2-like phenotype to a pro-inflammatory, anti-tumoral M1-like phenotype.[76–78] However, systemic administration of TLR agonists is limited clinically by severe side effects, notably cytokine storm.[79] Therefore, strategies enabling targeted release of TLR agonists have shown great potential to confine immune activation to the tumor site and reduce systemic toxicity.[80–85] Herein, we leverage our sono-responsive DHBC platform to precisely control the release of the TLR agonist (R848) under LITUS. Our pro-agonist, **ProR848**, demonstrates outstanding biocompatibility towards TAMs, exhibiting negligible toxicity at 10 μM (**Figure S19a**). Evaluation of inflammatory markers CD86 and CD80 revealed that TAMs activation by 1 μM **ProR848** was minimal (**Figure S19b**,**c**), indicating its potential for minimizing systemic immune activation. Subsequent LITUS-mediated activation of 1 μM **ProR848** was monitored using HPLC (Figure 6a). Ultrasonicated samples exhibited a distinct chromatographic peak at approximately 6.6 mins (**Figure S20**), indicative of the release of active R848 cargos. R848 release peaked at approximately 0.07 μM within the first three minutes of sonication and subsequently decreased upon prolonged irradiation (**Figure 6a**).

Having confirmed LITUS-triggered R848 release, we evaluated its ability to induce TAMs polarization. PBS-treated and 0.07 μM R848-treated groups served as negative and positive controls, respectively. Flow cytometric analysis demonstrated that ultrasound-activated **ProR848** (G4, orange bars) significantly upregulated pro-inflammatory markers CD86, CD80, and inducible nitric oxide synthase (iNOS) in TAMs, mirroring the response elicited by free R848 (G2) treatment (**Figure 6b–d**). In contrast, TAMs exposed to non-sonicated ProR848 (G3) exhibited marker expression comparable to PBS controls (G1), demonstrating that the TAMs polarization was due to LITUS-mediated drug release. Additionally, a substantial enhancement in major histocompatibility complex class II (MHCII) expression endowed macrophages with augmented antigen-presenting capabilities, facilitating improved activation and maturation of CD4⁺ helper T cells and subsequent adaptive

View Article Online
DOI: 10.1039/D5SC05710H

immune responses (**Figure 6e**).[86,87] The immunostimulatory efficacy of **ProR848** under LITUS irradiation was further corroborated by enzyme-linked immunosorbent assay (ELISA) data, revealing significantly elevated secretion of proinflammatory cytokines tumor necrosis factor-alpha (TNF-α) and interleukin-6 (IL-6) following ultrasound treatment (**Figure 6f,g**).

Dendritic cells (DCs) are another immune cell type with important roles in orchestrating innate and adaptive immunity. We further evaluated the effects of ultrasound-activated **ProR848** on DC maturation using the DC2.4 cell line. Similar to TAMs, DC2.4 cells exhibited excellent tolerance to 1 μM **ProR848**, without evidence of DCs maturation (**Figure S21 a,b**). Remarkably, upon ultrasound exposure, significant maturation of DC2.4 cells was observed, as evidenced by pronounced increases in MHCII expression (**Figure S21c**). Collectively, our results demonstrate that LITUS-triggered R848 release from **ProR848** effectively activates TAMs and promotes DCs maturation. This strategy enables on-demand and localized immune cell activation and holds promise for targeted immunotherapy with reduced systemic immune-related adverse effects.

Conclusions

This work introduces a sonochemical strategy to control prodrug activation through ultrasound-triggered cleavage of a DHBC prodrug platform. Using a commercially available, FDA-registered therapeutic ultrasound device, we demonstrated that our standard LITUS conditions generate ·OH radicals at a rate of several μM/min. The DHBC prodrug scaffold is designed to undergo radical hydroxylation by these sonochemically generated ·OH radicals, triggering a self-immolative cascade to release the cargo molecule. Using a chemotherapy prodrug model **ProDOX** as a proof-of-concept, we show that LITUS irradiation triggers DOX release, effectively killing *HeLa* cells in vitro. Notably, sonochemical manipulation of the DHBC prodrugs was successfully achieved through a layer of chicken breast, highlighting the deep-penetration capability of our approach. Moreover, to address systemic toxicity associated with TLR agonists in immunotherapy, we developed a LITUS-activable prodrug **ProR848**. Upon LITUS activation, **ProR848** released R848 and induced the polarization of TAMs and maturation of DC cells, demonstrating the potential to trigger localized immunostimulatory activity through our sonochemical strategy. Together, these results demonstrate the versatility of our sonochemical cleavage platform for controlled release of chemotherapy and immunomodulatory drugs, offering potential for targeted delivery in deep tissues inaccessible by conventional noninvasive stimuli. Future work will focus on understanding structure-sonochemical reactivity relationships in bioactive substances and designing prodrug molecules with enhanced resistance to unspecific sonolysis.

Ethical statements

All experimental procedures, including chemical synthesis, analytical measurements, cell culture studies, and experiments with chicken breast tissue were conducted in compliance with the relevant national regulations and institutional guidelines at Syracuse University (approval committees include the Environmental Health and Safety Services, the Institutional Biosafety Committee, and the Institutional Animal Care and Use Committee).

Author contributions

X. Fu led the study and contributed to the manuscript writing. B. Xu, H. Liyanage, C. Zhang, W. F. Kincaid, A. L. Ford, L. G. Westbrook, S. D. Brown, and T. DeMarco contributed to the experimental work. J. L. Hougland and J. M. Franck supervised students and provided research resources. X. Hu conceived and oversaw the project, secured funding and resources, and contributed to the manuscript writing.

Conflicts of interest

There are no conflicts to declare.

Data availability

The Supporting Information is available free of charge online. Experimental details, supporting figures, synthetic procedures, UV–vis, fluorescence, HPLC, and NMR spectra.

Acknowledgements

Financial support from Syracuse University (SU) is gratefully acknowledged. JLH acknowledges financial support from NIH grant GM134102.
The authors acknowledge that elements of Figure 1 and the TOC graphic were created with BioRender.com (Created in BioRender. Fu, X. (2025) https://BioRender.com/iyp1wme.

References

(1) Kost, J.; Langer, R. Responsive Polymer Systems for Controlled Delivery of Therapeutics. *Trends in Biotechnology* **1992**, *10*, 127–131. https://doi.org/10.1016/0167-7799(92)90194-Z.
(2) Mura, S.; Nicolas, J.; Couvreur, P. Stimuli-Responsive Nanocarriers for Drug Delivery. *Nature Mater* **2013**, *12* (11), 991–1003. https://doi.org/10.1038/nmat3776.
(3) Wang, J.; Wang, X.; Fan, X.; Chen, P. R. Unleashing the Power of Bond Cleavage Chemistry in Living Systems. *ACS Cent. Sci.* **2021**, *7* (6), 929–943. https://doi.org/10.1021/acscentsci.1c00124.
(4) Dvir, T.; Banghart, M. R.; Timko, B. P.; Langer, R.; Kohane, D. S. Photo-Targeted Nanoparticles. *Nano Lett.* **2010**, *10* (1), 250–254. https://doi.org/10.1021/nl903411s.
(5) Velema, W. A.; Szymanski, W.; Feringa, B. L. Photopharmacology: Beyond Proof of Principle. *J. Am. Chem. Soc.* **2014**, *136* (6), 2178–2191. https://doi.org/10.1021/ja413063e.

(6) Fu, Q.; Zhang, S.; Shen, S.; Gu, Z.; Chen, J.; Song, D.; Sun, P.; Wang, C.; Guo, Z.; Xiao, Y.; Gao, Y. Q.; Guo, Z.; Liu, Z. Radiotherapy-Triggered Reduction of Platinum-Based Chemotherapeutic Prodrugs in Tumours. *Nat. Biomed. Eng* **2024**, *8* (11), 1425–1435. https://doi.org/10.1038/s41551-024-01239-x.

(7) Fu, Q.; Gu, Z.; Shen, S.; Bai, Y.; Wang, X.; Xu, M.; Sun, P.; Chen, J.; Li, D.; Liu, Z. Radiotherapy Activates Picolinium Prodrugs in Tumours. *Nat. Chem.* **2024**, *16* (8), 1348–1356. https://doi.org/10.1038/s41557-024-01501-4.

(8) Cui, X.-Y.; Li, Z.; Kong, Z.; Liu, Y.; Meng, H.; Wen, Z.; Wang, C.; Chen, J.; Xu, M.; Li, Y.; Gao, J.; Zhu, W.; Hao, Z.; Huo, L.; Liu, S.; Yang, Z.; Liu, Z. Covalent Targeted Radioligands Potentiate Radionuclide Therapy. *Nature* **2024**, *630* (8015), 206–213. https://doi.org/10.1038/s41586-024-07461-6.

(9) Lakshmanan, A.; Jin, Z.; Nety, S. P.; Sawyer, D. P.; Lee-Gosselin, A.; Malounda, D.; Swift, M. B.; Maresca, D.; Shapiro, M. G. Acoustic Biosensors for Ultrasound Imaging of Enzyme Activity. *Nat Chem Biol* **2020**, *16* (9), 988–996. https://doi.org/10.1038/s41589-020-0591-0.

(10) Wu, Y.; Liu, Y.; Huang, Z.; Wang, X.; Jin, Z.; Li, J.; Limsakul, P.; Zhu, L.; Allen, M.; Pan, Y.; Bussell, R.; Jacobson, A.; Liu, T.; Chien, S.; Wang, Y. Control of the Activity of CAR-T Cells within Tumours via Focused Ultrasound. *Nat Biomed Eng* **2021**, *5* (11), 1336–1347. https://doi.org/10.1038/s41551-021-00779-w.

(11) Bar-Zion, A.; Nourmahnad, A.; Mittelstein, D. R.; Shivaei, S.; Yoo, S.; Buss, M. T.; Hurt, R. C.; Malounda, D.; Abedi, M. H.; Lee-Gosselin, A.; Swift, M. B.; Maresca, D.; Shapiro, M. G. Acoustically Triggered Mechanotherapy Using Genetically Encoded Gas Vesicles. *Nat. Nanotechnol.* **2021**, *16* (12), 1403–1412. https://doi.org/10.1038/s41565-021-00971-8.

(12) Sawyer, D. P.; Bar-Zion, A.; Farhadi, A.; Shivaei, S.; Ling, B.; Lee-Gosselin, A.; Shapiro, M. G. Ultrasensitive Ultrasound Imaging of Gene Expression with Signal Unmixing. *Nat Methods* **2021**, *18* (8), 945–952. https://doi.org/10.1038/s41592-021-01229-w.

(13) Castle, J.; Butts, M.; Healey, A.; Kent, K.; Marino, M.; Feinstein, S. B. Ultrasound-Mediated Targeted Drug Delivery: Recent Success and Remaining Challenges. *American Journal of Physiology-Heart and Circulatory Physiology* **2013**, *304* (3), H350–H357. https://doi.org/10.1152/ajpheart.00265.2012.

(14) Fu, X.; Hu, X. Ultrasound-Controlled Prodrug Activation: Emerging Strategies in Polymer Mechanochemistry and Sonodynamic Therapy. *ACS Appl. Bio Mater.* **2024**, acsabm.4c00150. https://doi.org/10.1021/acsabm.4c00150.

(15) Wang, W.; Wu, X.; Kevin Tang, K. W.; Pyatnitskiy, I.; Taniguchi, R.; Lin, P.; Zhou, R.; Capocyan, S. L. C.; Hong, G.; Wang, H. Ultrasound-Triggered In Situ Photon Emission for Noninvasive Optogenetics. *J. Am. Chem. Soc.* **2023**, *145* (2), 1097–1107. https://doi.org/10.1021/jacs.2c10666.

(16) Lyu, Y.; Li, Q.; Xie, S.; Zhao, Z.; Ma, L.; Wu, Z.; Bao, W.; Cai, Y.; Liu, H.; He, H.; Xie, K.; Gao, F.; Yang, Y.; Wu, P.; He, P.; Wang, K.; Dai, X.; Wu, H.; Lan, T.; Cheng, C. Synergistic Ultrasound-Activable Artificial Enzyme and Precision Gene Therapy to Suppress Redox Homeostasis and Malignant Phenotypes for Controllably Combating Hepatocellular Carcinoma. *J. Am. Chem. Soc.* **2025**, *147* (3), 2350–2368. https://doi.org/10.1021/jacs.4c10997.

(17) Chen, F.; Ren, S.; Huang, L.; Wu, Q.; Li, M.; Li, S.; Gao, J.; Lai, Y.; Cai, Z.; Liu, X.; Tao, W.; Lammers, T.; Xu, Z.; Yu, H. Ultrasound-Activatable Lipid Nanoplatform for Region-Confined Innate Immune Stimulation and mRNA Vaccination Therapy of Cancer. *J. Am. Chem. Soc.* **2025**, https://doi.org/10.1021/jacs.5c06028.

(18) Wu, Z.; Zhang, L.; Wang, Z.; Liu, S.; Zhang, Q.; Shi, C.; Wang, Y.; Xu, G.; Zhu, D.; Bryce, M. R.; Ren, L.; Tang, B. Z. Sonodynamic and Bioorthogonal Sonocatalytic Thrombotic Therapy Based on AIE Cationic Tetranuclear Ir(III) Complex Nanoplatform Guided by NIR-Chemiluminescence Imaging. *Advanced Materials n/a* (n/a), 2503599. https://doi.org/10.1002/adma.202503599.

(19) Liu, S.; Li, J.; Wang, A.; Ng, D. K. P.; Zheng, N. Multicomponent Polymerization toward Poly(BODIPY-Sulfonamide)s as Unique SO2 Generators for Sonodynamic and Gas Combination Therapy. *Angewandte Chemie International Edition* **2025**, *64* (13), e202422362. https://doi.org/10.1002/anie.202422362.

(20) Yang, Z.; Jiao, Z.; Chen, Z.; Qiao, C.; Huang, C.; Wang, L.; Rao, Z.; Zhang, R.; Wang, Z. Programmable Bacterial Architects Crafting Sonosensitizers for Tumor-Specific Sonodynamic Immunotherapy. *Advanced Materials* **2025**, *37* (32), 2504206. https://doi.org/10.1002/adma.202504206.

(21) He, M.; Ma, Z.; Zhang, L.; Zhao, Z.; Zhang, Z.; Liu, W.; Wang, R.; Fan, J.; Peng, X.; Sun, W. Sonoinduced Tumor Therapy and Metastasis Inhibition by a Ruthenium Complex with Dual Action: Superoxide Anion Sensitization and Ligand Fracture. *J. Am. Chem. Soc.* **2024**, *146* (37), 25764–25779. https://doi.org/10.1021/jacs.4c08278.

(22) Yu, J.; He, S.; Zhang, C.; Xu, C.; Huang, J.; Xu, M.; Pu, K. Polymeric STING Pro-Agonists for Tumor-Specific Sonodynamic Immunotherapy. *Angewandte Chemie International Edition* **2023**, *62* (32), e202307272. https://doi.org/10.1002/anie.202307272.

(23) Wu, J.; Pu, K. Leveraging Semiconducting Polymer Nanoparticles for Combination Cancer Immunotherapy. *Advanced Materials* **2024**, *36* (1), 2308924. https://doi.org/10.1002/adma.202308924.

(24) Zhang, C.; Huang, J.; Zeng, Z.; He, S.; Cheng, P.; Li, J.; Pu, K. Catalytical Nano-Immunocomplexes for Remote-Controlled Sono-Metabolic Checkpoint Trimodal Cancer Therapy. *Nat Commun* **2022**, *13* (1), 3468. https://doi.org/10.1038/s41467-022-31044-6.

(25) Liu, L.; Zhang, J.; An, R.; Xue, Q.; Cheng, X.; Hu, Y.; Huang, Z.; Wu, L.; Zeng, W.; Miao, Y.; Li, J.; Zhou, Y.; Chen, H.-Y.; Liu, H.; Ye, D. Smart Nanosensitizers for Activatable Sono-Photodynamic Immunotherapy of Tumors by Redox-Controlled Disassembly. *Angewandte Chemie International Edition* **2023**, *62* (10), e202217055. https://doi.org/10.1002/anie.202217055.

(26) Xu, H.; Zheng, M.; Ye, D.; An, J.; Liu, Z.; Tang, Z.; Chen, X. Ultrasound-Triggered Activation of p-Azidobenzyloxycarbonyl-Based Prodrugs via Radical-Mediated Cascade Elimination. *J. Am. Chem. Soc.* **2025**, *147* (24), 20667–20679. https://doi.org/10.1021/jacs.5c03878.

(27) Hu, X.; Zeng, T.; Husic, C. C.; Robb, M. J. Mechanically Triggered Small Molecule Release from a Masked Furfuryl Carbonate. *J. Am. Chem. Soc.* **2019**, *141* (38), 15018–15023. https://doi.org/10.1021/jacs.9b08663.

(28) Hu, X.; Zeng, T.; Husic, C. C.; Robb, M. J. Mechanically Triggered Release of Functionally Diverse Molecular Payloads from Masked 2-Furylcarbinol Derivatives. *ACS Cent. Sci.* **2021**, *7* (7), 1216–1224. https://doi.org/10.1021/acscentsci.1c00460.

(29) Huo, S.; Zhao, P.; Shi, Z.; Zou, M.; Yang, X.; Warszawik, E.; Loznik, M.; Göstl, R.; Herrmann, A. Mechanochemical Bond Scission for the Activation of Drugs. *Nat. Chem.* **2021**, *13* (2), 131–139. https://doi.org/10.1038/s41557-020-00624-8.

(30) Kim, G.; Wu, Q.; Chu, J. L.; Smith, E. J.; Oelze, M. L.; Moore, J. S.; Li, K. C. Ultrasound Controlled Mechanophore Activation in Hydrogels for Cancer Therapy. *Proceedings of the National Academy of Sciences* **2022**, *119* (4), e2109791119. https://doi.org/10.1073/pnas.2109791119.

(31) Sun, Y.; Neary, W. J.; Burke, Z. P.; Qian, H.; Zhu, L.; Moore, J. S. Mechanically Triggered Carbon Monoxide Release with Turn-On Aggregation-Induced Emission. *J. Am. Chem. Soc.* **2022**, *144* (3), 1125–1129. https://doi.org/10.1021/jacs.1c12108.

(32) Chen, L.; Nixon, R.; De Bo, G. Force-Controlled Release of Small Molecules with a Rotaxane Actuator. *Nature* **2024**, *628* (8007), 320–325. https://doi.org/10.1038/s41586-024-07154-0.

(33) Versaw, B. A.; Zeng, T.; Hu, X.; Robb, M. J. Harnessing the Power of Force: Development of Mechanophores for Molecular Release. *J. Am. Chem. Soc.* **2021**, *143* (51), 21461–21473. https://doi.org/10.1021/jacs.1c11868.

(34) Yao, Y.; McFadden, M. E.; Luo, S. M.; Barber, R. W.; Kang, E.; Bar-Zion, A.; Smith, C. A. B.; Jin, Z.; Legendre, M.; Ling, B.; Malounda, D.; Torres, A.; Hamza, T.; Edwards, C. E. R.; Shapiro, M. G.; Robb, M. J. Remote Control of Mechanochemical Reactions under Physiological Conditions Using Biocompatible Focused Ultrasound. *Proceedings of the National Academy of Sciences* **2023**, *120* (39), e2309822120. https://doi.org/10.1073/pnas.2309822120.

(35) Ishaqat, A.; Hahmann, J.; Lin, C.; Zhang, X.; He, C.; Rath, W. H.; Habib, P.; Sahnoun, S. E. M.; Rahimi, K.; Vinokur, R.; Mottaghy, F. M.; Göstl, R.; Bartneck, M.; Herrmann, A. In Vivo Polymer Mechanochemistry with Polynucleotides. *Advanced Materials* **2024**, *36* (32), 2403752. https://doi.org/10.1002/adma.202403752.

(36) Fan, J.; Lennarz, R.; Zhang, K.; Mourran, A.; Meisner, J.; Xuan, M.; Göstl, R.; Herrmann, A. Polymer Microbubbles as Universal Platform to Accelerate Polymer Mechanochemistry. *Nat Commun* **2025**, *16* (1), 5380. https://doi.org/10.1038/s41467-025-60667-8.

(37) Suslick, K. S.; Price, G. J. APPLICATIONS OF ULTRASOUND TO MATERIALS CHEMISTRY. *Annu. Rev. Mater. Sci.* **1999**, *29* (1), 295–326. https://doi.org/10.1146/annurev.matsci.29.1.295.

(38) Henglein, A. Sonochemistry: Historical Developments and Modern Aspects. *Ultrasonics* **1987**, *25* (1), 6–16. https://doi.org/10.1016/0041-624X(87)90003-5.

(39) Mišík, V.; Riesz, P. Free Radical Intermediates in Sonodynamic Therapy. *Annals of the New York Academy of Sciences* **2000**, *899* (1), 335–348. https://doi.org/10.1111/j.1749-6632.2000.tb06198.x.

(40) Christman, C. L.; Carmichael, A. J.; Mossoba, M. M.; Riesz, P. Evidence for Free Radicals Produced in Aqueous Solutions by Diagnostic Ultrasound. *Ultrasonics* **1987**, *25* (1), 31–34. https://doi.org/10.1016/0041-624X(87)90008-4.

(41) Juffermans, L. J. M.; Dijkmans, P. A.; Musters, R. J. P.; Visser, C. A.; Kamp, O. Transient Permeabilization of Cell Membranes by Ultrasound-Exposed Microbubbles Is Related to Formation of Hydrogen Peroxide. *American Journal of Physiology-Heart and Circulatory Physiology* **2006**, *291* (4), H1595–H1601. https://doi.org/10.1152/ajpheart.01120.2005.

(42) Riesz, P.; Berdahl, D.; Christman, C. L. Free Radical Generation by Ultrasound in Aqueous and Nonaqueous Solutions. *Environmental Health Perspectives* **1985**, *64*, 233–252. https://doi.org/10.1289/ehp.8564233.

(43) Martínez, R. F.; Cravotto, G.; Cintas, P. Organic Sonochemistry: A Chemist's Timely Perspective on Mechanisms and Reactivity. *J. Org. Chem.* **2021**, *86* (20), 13833–13856. https://doi.org/10.1021/acs.joc.1c00805.

(44) Sazgarnia, A.; Shanei, A.; Eshghi, H.; Hassanzadeh-Khayyat, M.; Esmaily, H.; Shanei, M. M. Detection of Sonoluminescence Signals in a Gel Phantom in the Presence of Protoporphyrin IX Conjugated to Gold Nanoparticles. *Ultrasonics* **2013**, *53* (1), 29–35. https://doi.org/10.1016/j.ultras.2012.03.009.

(45) He, Y.; Xing, D.; Tan, S.; Tang, Y.; Ueda, K. In Vivo Sonoluminescence Imaging with the Assistance of FCLA. *Phys. Med. Biol.* **2002**, *47* (9), 1535–1541. https://doi.org/10.1088/0031-9155/47/9/308.

(46) He, Y.; Xing, D.; Yan, G.; Ueda, K. FCLA Chemiluminescence from Sonodynamic Action in Vitro and in Vivo. *Cancer Letters* **2002**, *182* (2), 141–145. https://doi.org/10.1016/S0304-3835(02)00070-8.

(47) Makino, K.; Mossoba, M. M.; Riesz, P. Formation of · OH and · H in Aqueous Solutions by Ultrasound Using Clinical Equipment. *Radiation Research* **1983**, *96* (2), 416. https://doi.org/10.2307/3576225.

(48) Suslick, K. S. Sonochemistry. *Science* **1990**, *247* (4949), 1439–1445. https://doi.org/10.1126/science.247.4949.1439.

(49) Suslick, K. S.; Doktycz, S. J.; Flint, E. B. On the Origin of Sonoluminescence and Sonochemistry. *Ultrasonics* **1990**, *28* (5), 280–290. https://doi.org/10.1016/0041-624X(90)90033-K.

(50) *Sonochemistry and Sonoluminescence*; Crum, L. A., Mason, T. J., Reisse, J. L., Suslick, K. S., Eds.; Springer Netherlands: Dordrecht, 1999. https://doi.org/10.1007/978-94-015-9215-4.

(51) Miyoshi, N.; Igarashi, T.; Riesz, P. Evidence against Singlet Oxygen Formation by Sonolysis of Aqueous Oxygen-Saturated Solutions of Hematoporphyrin and Rose Bengal. *Ultrasonics Sonochemistry* **2000**, *7* (3), 121–124. https://doi.org/10.1016/S1350-4177(99)00042-5.

(52) Mišík, V.; Miyoshi, N.; Riesz, P. EPR Spin Trapping Study of the Decomposition of Azo Compounds in Aqueous Solutions by Ultrasound: Potential for Use as Sonodynamic Sensitizers for Cell Killing. *Free Radical Research* **1996**, *25* (1), 13–22. https://doi.org/10.3109/10715769609145652.

(53) Mišík, V.; Riesz, P. Recent Applications of EPR and Spin Trapping to Sonochemical Studies of Organic Liquids and Aqueous Solutions. *Ultrasonics Sonochemistry* **1996**, *3* (3), S173–S186. https://doi.org/10.1016/S1350-4177(96)00023-5.

(54) Mead, E. L.; Sutherland, R. G.; Verrall, R. E. Ultrasonic Degradation of Thymine. *J. Chem. Soc., Chem. Commun.* **1973**, No. 13, 414. https://doi.org/10.1039/c39730000414.

(55) Okitsu, K.; Ashokkumar, M.; Grieser, F. Sonochemical Synthesis of Gold Nanoparticles: Effects of Ultrasound Frequency. *J. Phys. Chem. B* **2005**, *109* (44), 20673–20675. https://doi.org/10.1021/jp0549374.

(56) Bradley, M.; Ashokkumar, M.; Grieser, F. Sonochemical Production of Fluorescent and Phosphorescent Latex Particles. *J. Am. Chem. Soc.* **2003**, *125* (2), 525–529. https://doi.org/10.1021/ja0268581.

(57) Vinodgopal, K.; Ashokkumar, M.; Grieser, F. Sonochemical Degradation of a Polydisperse Nonylphenol Ethoxylate in Aqueous Solution. *J. Phys. Chem. B* **2001**, *105* (16), 3338–3342. https://doi.org/10.1021/jp004178j.

(58) Berlan, J.; Trabelsi, F.; Delmas, H.; Wilhelm, A. M.; Petrignani, J. F. Oxidative Degradation of Phenol in Aqueous Media Using Ultrasound. *Ultrasonics Sonochemistry* **1994**, *1* (2), S97–S102. https://doi.org/10.1016/1350-4177(94)90005-1.

(59) Weissler, A. Ultrasonic Hydroxylation in a Fluorescence Analysis for Microgram Quantities of Benzoic Acid. *Nature* **1962**, *193* (4820), 1070–1070. https://doi.org/10.1038/1931070a0.

(60) Ashokkumar, M.; Sunartio, D.; Kentish, S.; Mawson, R.; Simons, L.; Vilkhu, K.; Versteeg, C. (Kees). Modification of Food Ingredients by Ultrasound to Improve Functionality: A Preliminary Study on a Model System. *Innovative Food Science & Emerging Technologies* **2008**, *9* (2), 155–160. https://doi.org/10.1016/j.ifset.2007.05.005.

(61) Tong, Y.; Li, M.; Huang, H.; Long, S.; Sun, W.; Du, J.; Fan, J.; Wang, L.; Liu, B.; Peng, X. Urea-Bond Scission Induced by Therapeutic Ultrasound for Biofunctional Molecule Release. *J. Am. Chem. Soc.* **2022**, *144* (37), 16799–16807. https://doi.org/10.1021/jacs.2c03669.

(62) Anbar, M.; Meyerstein, D.; Neta, P. The Reactivity of Aromatic Compounds toward Hydroxyl Radicals. *J. Phys. Chem.* **1966**, *70* (8), 2660–2662. https://doi.org/10.1021/j100880a034.

(63) Kaur, H.; Halliwell, B. [6] Detection of Hydroxyl Radicals by Aromatic Hydroxylation. In *Methods in Enzymology*; Elsevier, 1994; Vol. 233, pp 67–82. https://doi.org/10.1016/S0076-6879(94)33009-3.

(64) Kurata, Tsunehiko.; Watanabe, Yasumasa.; Katoh, Makoto.; Sawaki, Yasuhiko. Mechanism of Aromatic Hydroxylation in the Fenton and Related Reactions. One-Electron Oxidation and the NIH Shift. *J. Am. Chem. Soc.* **1988**, *110* (22), 7472–7478. https://doi.org/10.1021/ja00230a032.

(65) Fu, Q.; Li, H.; Duan, D.; Wang, C.; Shen, S.; Ma, H.; Liu, Z. External-Radiation-Induced Local Hydroxylation Enables Remote Release of Functional Molecules in Tumors. *Angew Chem Int Ed* **2020**, *59* (48), 21546–21552. https://doi.org/10.1002/anie.202005612.

(66) Albarran, G.; Mendoza, E.; Schuler, R. H. Concerted Effects of Substituents in the Reaction of •OH Radicals with Aromatics: The Hydroxybenzaldehydes. *Radiation Physics and Chemistry* **2016**, *124*, 46–51. https://doi.org/10.1016/j.radphyschem.2015.11.022.

(67) Pan, X.-M.; Schuchmann, M. N.; Von Sonntag, C. Oxidation of Benzene by the OH Radical. A Product and Pulse Radiolysis Study in Oxygenated Aqueous Solution. *J. Chem. Soc., Perkin Trans. 2* **1993**, No. 3, 289. https://doi.org/10.1039/p29930000289.

(68) Jackson, S. K.; Thomas, M. P.; Smith, S.; Madhani, M.; Rogers, S. C.; James, P. E. In Vivo EPR Spectroscopy: Biomedical and Potential Diagnostic Applications. *Faraday Discuss.* **2004**, *126* (0), 103–117. https://doi.org/10.1039/B307162F.

(69) Mason, T. J.; Lorimer, J. P.; Bates, D. M.; Zhao, Y. Dosimetry in Sonochemistry: The Use of Aqueous Terephthalate Ion as a Fluorescence Monitor. *Ultrasonics Sonochemistry* **1994**, *1* (2), S91–S95. https://doi.org/10.1016/1350-4177(94)90004-3.

(70) Rajamma, D. B.; Anandan, S.; Yusof, N. S. M.; Pollet, B. G.; Ashokkumar, M. Sonochemical Dosimetry: A Comparative Study of Weissler, Fricke and Terephthalic Acid Methods. *Ultrasonics Sonochemistry* **2021**, *72*, 105413. https://doi.org/10.1016/j.ultsonch.2020.105413.

(71) Fang, X.; Mark, G.; von Sonntag, C. OH Radical Formation by Ultrasound in Aqueous Solutions Part I: The Chemistry Underlying the Terephthalate Dosimeter. *Ultrasonics Sonochemistry* **1996**, *3* (1), 57–63. https://doi.org/10.1016/1350-4177(95)00032-1.

(72) Tampieri, F.; Ginebra, M.-P.; Canal, C. Quantification of Plasma-Produced Hydroxyl Radicals in Solution and Their Dependence on the pH. *Anal. Chem.* **2021**, *93* (8), 3666–3670. https://doi.org/10.1021/acs.analchem.0c04906.

(73) Smith, J. D.; Kinney, H.; Anastasio, C. Aqueous Benzene-Diols React with an Organic Triplet Excited State and Hydroxyl Radical to Form Secondary Organic Aerosol. *Phys. Chem. Chem. Phys.* **2015**, *17* (15), 10227–10237. https://doi.org/10.1039/C4CP06095D.

(74) *Applications and clinical trial landscape using Toll-like receptor agonists to reduce the toll of cancer | npj Precision Oncology*. https://www.nature.com/articles/s41698-023-00364-1 (accessed 2025-06-30).

(75) Bhagchandani, S.; Johnson, J. A.; Irvine, D. J. Evolution of Toll-like Receptor 7/8 Agonist Therapeutics and Their Delivery Approaches: From Antiviral Formulations to Vaccine Adjuvants. *Advanced Drug Delivery Reviews* **2021**, *175*, 113803. https://doi.org/10.1016/j.addr.2021.05.013.

(76) Zhang, W.; Wang, M.; Ji, C.; Liu, X.; Gu, B.; Dong, T. Macrophage Polarization in the Tumor Microenvironment: Emerging Roles and Therapeutic Potentials. *Biomedicine & Pharmacotherapy* **2024**, *177*, 116930. https://doi.org/10.1016/j.biopha.2024.116930.

(77) Rodell, C. B.; Arlauckas, S. P.; Cuccarese, M. F.; Garris, C. S.; Li, R.; Ahmed, M. S.; Kohler, R. H.; Pittet, M. J.; Weissleder, R. TLR7/8-Agonist-Loaded Nanoparticles Promote the Polarization of Tumour-Associated Macrophages to Enhance Cancer Immunotherapy. *Nat Biomed Eng* **2018**, *2* (8), 578–588. https://doi.org/10.1038/s41551-018-0236-8.

(78) Fu, X.; Huang, Y.; Zhao, H.; Zhang, E.; Shen, Q.; Di, Y.; Lv, F.; Liu, L.; Wang, S. Near-Infrared-Light Remote-Controlled Activation of Cancer Immunotherapy Using Photothermal Conjugated Polymer Nanoparticles. *Advanced Materials* **2021**, *33* (34), 2102570. https://doi.org/10.1002/adma.202102570.

(79) Nie, J.; Zhou, L.; Tian, W.; Liu, X.; Yang, L.; Yang, X.; Zhang, Y.; Wei, S.; Wang, D. W.; Wei, J. Deep Insight into Cytokine Storm: From Pathogenesis to Treatment. *Sig Transduct Target Ther* **2025**, *10* (1), 112. https://doi.org/10.1038/s41392-025-02178-y.

(80) Li, J.; Yu, X.; Jiang, Y.; He, S.; Zhang, Y.; Luo, Y.; Pu, K. Second Near-Infrared Photothermal Semiconducting Polymer Nanoadjuvant for Enhanced Cancer Immunotherapy. *Advanced Materials* **2021**, *33* (4), 2003458. https://doi.org/10.1002/adma.202003458.

(81) Jiang, Y.; Huang, J.; Xu, C.; Pu, K. Activatable Polymer Nanoagonist for Second Near-Infrared Photothermal Immunotherapy of Cancer. *Nat Commun* **2021**, *12* (1), 742. https://doi.org/10.1038/s41467-021-21047-0.

(82) Wan, J.; Ren, L.; Li, X.; He, S.; Fu, Y.; Xu, P.; Meng, F.; Xian, S.; Pu, K.; Wang, H. Photoactivatable Nanoagonists Chemically Programmed for Pharmacokinetic Tuning and in Situ Cancer Vaccination. *Proceedings of the National Academy of*

View Article Online
DOI: 10.1039/D5SC05710H

Sciences **2023**, *120* (8), e2210385120. https://doi.org/10.1073/pnas.2210385120.

(83) Shen, J.; Xu, B.; Zheng, Y.; Zhao, X.; Qi, H.; Tang, Y.; Lin, W.; Li, S.; Zhong, Z. Near-Infrared Light-Responsive Immunomodulator Prodrugs Rejuvenating Immune Microenvironment for "Cold" Tumor Photoimmunotherapy. *Angewandte Chemie International Edition* **2025**, *64* (22), e202425309. https://doi.org/10.1002/anie.202425309.

(84) Ding, Z.; Yin, X.; Zheng, Y.; Li, Y.; Ge, H.; Feng, J.; Wang, Z.; Qiao, S.; Sun, Q.; Yu, F.; Hou, Z.; Fu, Y.-X.; Liu, Z. Single Atom Engineering for Radiotherapy-Activated Immune Agonist Prodrugs. *Nat Commun* **2025**, *16* (1), 6021. https://doi.org/10.1038/s41467-025-60768-4.

(85) Yin, X.; Ding, Z.; Yu, L.; Zhang, X.; Gao, Y.; Li, Y.; Liu, Z.; Fu, Y.-X. Orchestrating Intratumoral DC-T Cell Immunity for Enhanced Tumor Control via Radiotherapy-Activated TLR7/8 Prodrugs in Mice. *Nat Commun* **2025**, *16* (1), 6020. https://doi.org/10.1038/s41467-025-60769-3.

(86) McDevitt, H. O. Discovering the Role of the Major Histocompatibility Complex in the Immune Response. *Annual Review of Immunology* **2000**, *18* (Volume 18, 2000), 1–17. https://doi.org/10.1146/annurev.immunol.18.1.1.

(87) Al-Daccak, R.; Mooney, N.; Charron, D. MHC Class II Signaling in Antigen-Presenting Cells. *Current Opinion in Immunology* **2004**, *16* (1), 108–113. https://doi.org/10.1016/j.coi.2003.11.006.

View Article Online
DOI: 10.1039/D5SC05710H

The data supporting this article have been included as part of the Supplementary Information.